View metadata, citation and similar papers at core.ac.uk
brought to you by CORE
provided by Carolina Digital Repository

A Screen for Mutations That Suppress the Phenotype of *Drosophila armadillo*, the β-Catenin Homolog

Rachel T. Cox,* Donald G. McEwen,† Denise L. Myster,† Robert J. Duronio,*,†,‡,§ Joseph Loureiro‡ and Mark Peifer*,†,‡

‡*Department of Biology*, **Curriculum in Genetics and Molecular Biology*, †*Lineberger Comprehensive Cancer Center and* §*Program in Molecular Biology and Biotechnology, University of North Carolina, Chapel Hill, North Carolina 27599-3280*

Manuscript received February 24, 2000
Accepted for publication April 13, 2000

ABSTRACT

During development signaling pathways coordinate cell fates and regulate the choice between cell survival or programmed cell death. The well-conserved Wingless/Wnt pathway is required for many developmental decisions in all animals. One transducer of the Wingless/Wnt signal is Armadillo/β-catenin. Drosophila Armadillo not only transduces Wingless signal, but also acts in cell-cell adhesion via its role in the epithelial adherens junction. While many components of both the Wingless/Wnt signaling pathway and adherens junctions are known, both processes are complex, suggesting that unknown components influence signaling and junctions. We carried out a genetic modifier screen to identify some of these components by screening for mutations that can suppress the *armadillo* mutant phenotype. We identified 12 regions of the genome that have this property. From these regions and from additional candidate genes tested we identified four genes that suppress *arm*: *dTCF*, *puckered*, *head involution defective* (*hid*), and *Dpresenilin*. We further investigated the interaction with *hid*, a known regulator of programmed cell death. Our data suggest that Wg signaling modulates Hid activity and that Hid regulates programmed cell death in a dose-sensitive fashion.

THE development of a fertilized egg into a multicellular organism requires coordination of many processes. Each cell must choose the proper cell fate and must also assume its place as part of an organized tissue. In addition, apoptosis (programmed cell death; PCD) plays an important role in shaping an organism by eliminating unneeded cells. One conserved pathway that directs cell fate decisions in many animals is the Wingless (Wg)/Wnt signal transduction pathway (proteins listed as X/Y represent nomenclature in Drosophila/mammals). Loss-of-function mutations in this pathway are lethal, while inappropriate activation can be oncogenic. Wg/Wnt signals are transduced by homologous components in Drosophila, Xenopus, and mammals (reviewed in Polakis 1999). During normal development, most cells do not receive Wg/Wnt signals. In these cells the pathway is kept off through the actions of several proteins, including Zestewhite3/GSK3β, the tumor-suppressor adenomatous polyposis coli, and axin, which work in conjunction to target Armadillo (Arm)/β-catenin (βcat) for degradation via the proteasome. Arm/βcat is thus the pivotal component in the pathway. When Wg/Wnt is absent, cytoplasmic levels of Arm/βcat are very low. However, Wg/Wnt signal relieves the destruction of Arm/βcat. Arm/βcat accumulates, translocates into the nucleus, and binds dTCF/TCF, forming a bipartite transcription factor that turns on Wg/Wnt-responsive genes.

The components of the Wg pathway are encoded by a subset of the segment polarity genes, mutations that affect cell fate in the embryonic epidermis. In normal fly embryos, anterior cells of each segment secrete denticles, while posterior cells secrete naked cuticle. Wg signal directs cells to choose posterior fates and thus secrete naked cuticle. In an embryo mutant for *wg* or other positively acting components of the Wg pathway, cell fates are altered such that all surviving cells secrete denticles. It is important to note, however, that in a *wg* mutant many epidermal cells fail to survive to secrete cuticle, instead undergoing PCD. Embryos mutant for genes in either the Wg or the Hedgehog pathways have elevated levels of epidermal PCD (Martinez Arias 1985; Klingensmith *et al.* 1989; Pazdera *et al.* 1998).

Arm's role in Wg signaling is not its only function. The earliest requirement for Arm is in cell adhesion (Cox *et al.* 1996). Arm/βcat is an essential component of epithelial cell-cell adherens junctions (reviewed in Provost and Rimm 1999). The core components of this junction are classic cadherins, transmembrane proteins that mediate homotypic adhesion between neighboring cells. Arm/βcat binds to the cadherin cytoplasmic tail. α-Catenin then binds to Arm/βcat, linking the actin cytoskeleton to adherens junctions. In Drosophila, Arm helps assemble adherens junctions very early during embryogenesis. This is initiated by maternal Arm, which is supplemented by zygotic Arm once transcription begins. If the embryo lacks maternal and zygotic Arm, it

Corresponding author: Mark Peifer, Biology, CB#3280, University of North Carolina, Chapel Hill, NC 27599-3280.
E-mail: peifer@unc.edu

does not form proper adherens junctions, and cells of the cellularized blastoderm cannot form epithelia (Cox *et al.* 1996). In addition to the essential role that Arm/βcat and adherens junctions play in embryogenesis, loss-of-function mutations in the cadherin-catenin system contribute to tumorigenicity, as tumor cells must alter their adhesive properties to metastasize.

While the roles of Arm/βcat in Wg/Wnt signaling and adherens junctions have become clearer, many questions remain concerning both processes. In addition, biochemical approaches identified many other proteins that bind βcat, perhaps implicating it in other functions: for example, Arm/βcat binds the epidermal growth factor (EGF) receptor at the cell surface (Hoschuetzky *et al.* 1994), the actin-binding protein fascin in the cortex (Tao *et al.* 1996), Presenilin proteins, presumably in the endoplasmic reticulum (ER) (Zhou *et al.* 1997; Yu *et al.* 1998), and the transcription factor Teashirt (Gallet *et al.* 1998). One strategy to identify novel proteins involved in cell adhesion and Wg signaling and simultaneously to search for biological functions of the interaction of Arm with other partners is to look for mutations that interact genetically with *arm*.

In designing such a genetic screen, we took advantage of Arm's dual roles in signaling and adhesion. It has been suggested that cells may use this coupling, allowing one process to regulate the other via competition for a limited pool of Arm. Although in wild-type Drosophila embryos more than enough Arm is synthesized to fulfill its roles in both signaling and adhesion, one can manipulate the pool of Arm to make signaling and adhesion competitive. For example, if one expresses excess cadherin, it titrates out all the Arm, leaving none available for Wg signaling and resulting in a segment polarity phenotype (Sanson *et al.* 1996). We utilized this balance between Arm assembled into adherens junctions and that remaining for Wg signaling to create a sensitized genetic background. We reduced the amount of available Arm until adhesion and Wg signaling became competitive by using a zygotic *arm* mutant that retains wild-type maternal Arm, sufficing for Arm's role in adherens junctions (Cox *et al.* 1996). With most wild-type maternal Arm assembled in adherens junctions, the embryo drops below the critical threshold of Arm necessary for Wg signaling, resulting in segment polarity defects. Such an embryo is very sensitive to slight changes in *arm* dose; for example, doubling the maternal Arm substantially suppresses the segment polarity phenotype (Wieschaus and Noell 1986). Thus this represents a sensitized background well suited for a modifier screen. Mutations in genes that affect adherens junction assembly, which negatively regulate Wg signaling or encode other proteins that bind the limited supply of maternal Arm, could all potentially suppress the segment polarity phenotype of *arm*. We previously demonstrated the feasibility of this idea, showing that reduction in DE-cadherin suppressed *arm*'s segment polarity phenotype (Cox *et al.* 1996).

We used the sensitized background of a zygotic *arm* mutant to carry out a modifier screen, looking for changes in the segment polarity phenotype. We screened through deficiencies covering >80% of the second, third, and fourth chromosomes, searching for regions of the genome containing a gene or genes that, when heterozygous deficient, suppress the cuticle phenotype of *arm*. We found 12 such regions and identified four genes with this property. One interactor is the PCD-promoting gene *head involution defective* (*hid*). Our data suggest that Hid acts as a dose-sensitive regulator of PCD in the ventral epidermis of segment polarity mutants.

MATERIALS AND METHODS

Fly stocks: References for mutants used were the following: arm^{XP33}, arm^{XM19}, and $zw3^{m1\text{-}1}arm^{XM19}$ (Cox *et al.* 1996; Peifer *et al.* 1994); hid^{05014} (Grether *et al.* 1995); hid^{WR+X1} (Abbott and Lengyel 1991); *Df(3)H99* (White *et al.* 1994); wg^{IG22} (Nüsslein-Volhard and Wieschaus 1980); UAS-p35 (Hay *et al.* 1994); other mutations, http://flybase.bio.indiana.edu/. The deficiency kits were from the Bloomington Drosophila Stock Center, the *P*-lethals from Bloomington or the Berkeley Drosophila Genome Project (BDGP), and the *Dpresenilin* alleles from D. Curtis.

Cuticle preparations and counting: Cuticle preparations were as in Wieschaus and Nüsslein-Volhard (1986). Care was taken to be consistent in cuticle preparations, as differences in baking and pressing alter cuticle appearance. If the first cross suggested an interaction, the cross was repeated. Each candidate interacting region was tested in two or more separate crosses, with ≥200 cuticles scored per cross. Percentage of suppression equaled the number of cuticles in the least severe classes divided by the total number of cuticles scored.

Terminal transferase dUTP nick end labeling (TUNEL), phalloidin and antibody staining: TUNEL was done using reagents from Boehringer Mannheim (Indianapolis). Embryos were dechorionated in 50% bleach, fixed in 1:1 4% formaldehyde:heptane for 30 min, hand devitellinized, rinsed once in TdT reaction buffer (2.5 mm $CoCl_2$, 1× transferase buffer), and reacted in TdT reaction mix (50 units terminal transferase, 2:1 10 μm final concentration of dUTP:dUTP-biotin in reaction buffer) for 3 hr at 37°. After washing three times for 10 min in PBS + 0.1% Triton X-100 (PBT), the end-labeling was first amplified using the Vectastain kit (Vector Labs, Burlingame, CA) as recommended by the manufacturer, amplified with Cy3tyramide (New England Nuclear, Boston), and washed three times for 10 min in PBT. BODIPY, phalloidin (Molecular Probes, Eugene, OR) was added during the avidin-biotin reaction of the first amplification. Antiphosphotyrosine labeling was as in Cox *et al.* (1996).

Phosphohistone H3 staining: The 2- to 7-hr-old embryos were dechorionated in 50% bleach, fixed in 1:1 5% formaldehyde:heptane for 20 min, blocked (50 mm Tris pH 7.4, 150 mm NaCl, 0.5% NP-40, 5 mg/ml BSA) at 4° for 2 hr and stained overnight at 4° with 1:1000 antiphosphohistone H3 (Upstate Biotechnology, Lake Placid, NY) and 1:500 anti-β-gal (Boehringer Mannheim, Indianapolis). Secondary antibodies were from Molecular Probes. Pictures of the ventral epidermis and dorsal germband were taken, mitotic figures (stained for phosphohistone H3) counted, and means and standard deviations calculated.

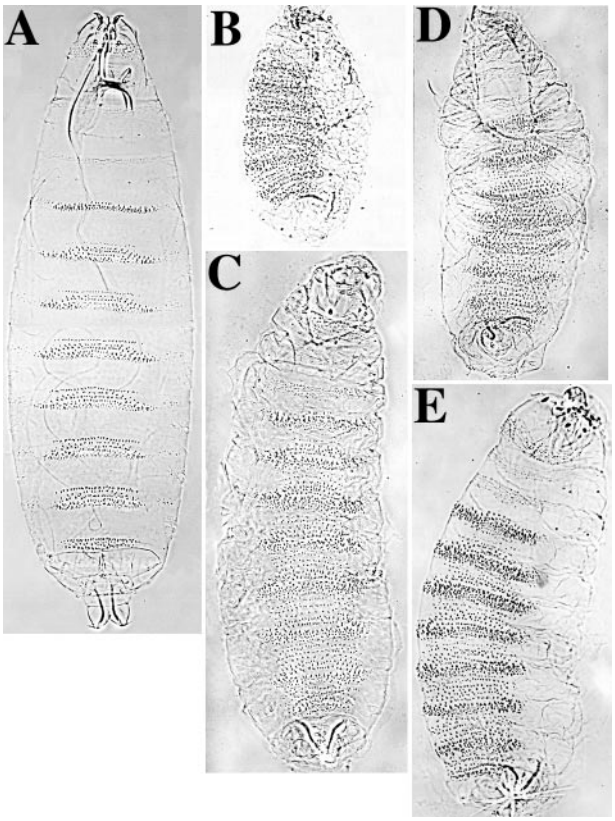

Figure 1.—Reducing dosage of DE-cadherin or Zw3 suppresses *arm*'s embryonic phenotype. (A) Wild-type cuticle. The cuticle is closed dorsally and the ventral surface has alternating belts of denticles and naked cuticle. (B) arm^{XP33}/Y. arm^{XP33} mutant cuticles are shorter than wild type, with a lawn of ventral denticles, no naked cuticle, and incomplete dorsal closure. (C) arm^{XP33}/*Y; Df(3) E2*/+. When the dose of DE-cadherin is reduced by half, the *arm* phenotype is suppressed. The cuticle is longer, the lawn of denticles is less dense, and the dorsal closure defect is rescued. (D) arm^{XM19}/Y, a somewhat weaker allele. (E) arm^{XM19} $zw3^{M1\text{-}1}$/Y. When zygotic *zw3* is removed (leaving only maternal *zw3*), the phenotype of arm^{XM19} is suppressed.

RESULTS

Strategy for the screen for modifiers: arm^{XP33} encodes a carboxy-terminally truncated Arm protein that cannot function in Wg signaling and has almost no function in adherens junctions (Cox *et al.* 1996). In an arm^{XP33} zygotic mutant, maternal wild-type Arm provides sufficient function for adherens junctions. However, as nearly all maternal Arm is recruited into junctions (Cox *et al.* 1996), little Arm remains to transduce Wg signal, resulting in a strong segment polarity phenotype (Figure 1, A *vs.* B). We reasoned that if one elevated the level or function of the limiting pool of maternal Arm, this should suppress the defect in Wg signaling. We hypothesized that this could occur by freeing maternal Arm from junctions, reducing the effectiveness of negative regulation of Arm's role in Wg signaling or by reducing the level of a distinct Arm-binding protein. Of course in genetic screens modifiers are also found that operate by unexpected mechanisms.

The feasibility of this hypothesis was supported by two observations. We previously found that heterozygosity for a chromosomal deficiency removing *DE-cadherin*, *Df(3R)E2*, suppresses the embryonic phenotype of arm^{XP33}—the cuticle is longer, the dorsal closure defect is substantially reduced, and denticle diversity is partially restored (Figure 1, B *vs.* C; Cox *et al.* 1996). We presume that reducing the gene dose of DE-cadherin by half creates an embryo with fewer Arm/Cadherin complexes. Although this has no apparent effect on cell-cell adhesion, wild-type maternal Arm is freed up to function in Wg signaling, leading to a suppressed phenotype. A similar suppression of *arm* was seen by removing the zygotic contribution of one of Arm's negative regulators, Zw3 (Figure 1, D *vs.* E; we tested this on arm^{XM19}, a less severe allele).

A modifier screen for Arm interactors: These examples demonstrated that a 50% reduction in the dose of certain genes suppresses *arm*. We thus screened for dose-sensitive modifiers. Rather than examining single genes one by one by mutagenesis, we evaluated large regions of the genome simultaneously by making animals heterozygous for chromosomal deficiencies that remove many genes. We obtained the "deficiency kits" for three of the four chromosomes from the Bloomington Drosophila Stock Center. These kits are designed to delete as much of the chromosome as possible using the fewest stocks; 70–80% of the euchromatin was covered by this collection of Deficiencies when we obtained them. We extended our analysis by obtaining additional Deficiencies that either covered regions not covered in the kit or overlapped interacting Deficiencies. We estimate we covered >80% of the autosomes. We have not examined the X chromosome thus far, as *arm* is on the X and the screen would require recombination of *arm* onto each deficiency. To carry out the screen, we crossed virgin arm^{XP33} females to males heterozygous for each Deficiency and prepared cuticles from the dead embryonic progeny (Figure 2A). One-quarter of the progeny are arm^{XP33}/Y (since *arm* is X-linked), and these die due to loss of *arm* function. Half of these embryos will be hemizygous for genes deleted by the deficiency and could potentially have a modified segment polarity phenotype.

To determine if there was an interaction, we grouped cuticles into phenotypic classes. arm^{XP33} mutants exhibit a segment polarity phenotype, with all surviving cells adopting anterior fates and secreting denticles. However, arm^{XP33} mutants show a range of severities; the phenotypes vary about a mean (Figure 2B). In embryos with the most severe phenotype (like that of the zygotic null), the cuticle is much shorter than the wild type and is open dorsally. In less severe embryos, dorsal closure is partially complete, and the embryonic cuticle is longer. Most mutant embryos fall into these classes. At a very

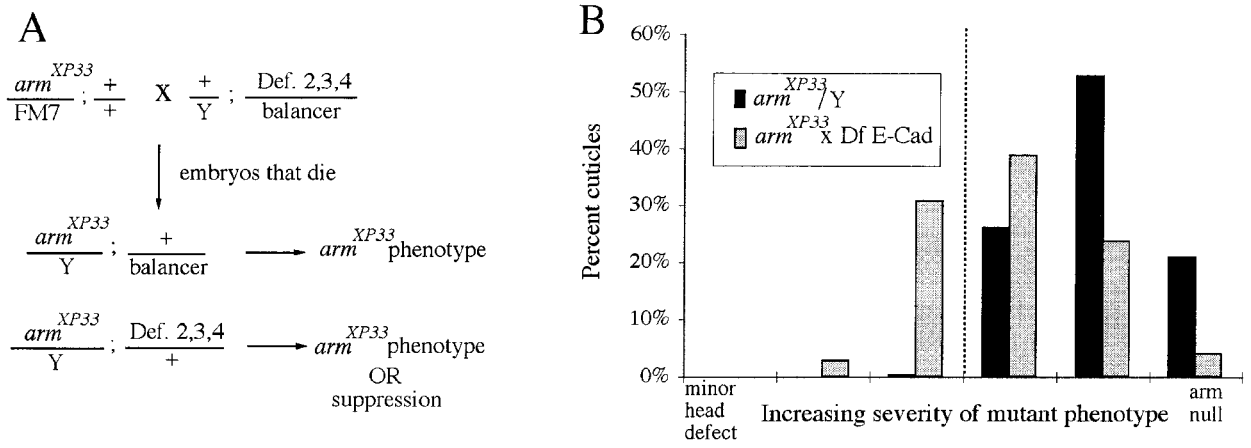

Figure 2.—Modifier screen strategy. (A) Cross scheme. arm^{XP33}/FM7 virgin females were crossed to males carrying a single deficiency on chromosome 2, 3, or 4. One-quarter of the progeny are arm^{XP33}/Y and die with a segment polarity phenotype. Half of these are heterozygous for the deficiency. Cuticles were prepared from dead embryonic progeny of each cross. If there is an interaction, these cuticles show suppression of *arm*. (B) The arm^{XP33} cuticle phenotype varies about a mean (black bars). Removing one copy of DE-cadherin shifts the distribution, greatly increasing the fraction with the least severe phenotypes (light bars). Our scoring scheme for phenotypic severity was based on cuticle size, strength of the segment polarity phenotype, and degree of dorsal closure. We counted ≥200 embryos per cross. Percentage of suppression = the number of progeny in the least severe classes (left of the dashed line) divided by the total number of progeny scored.

low frequency (0.5%), arm^{XP33}/Y cuticles have the least severe phenotype: these are nearly wild type in length, have greater denticle diversity, and are dorsally closed (they retain an anterior hole). If one does a similar analysis of arm^{XP33}/Y; *Df-DE-cadherin*/+ embryos, as an example of suppression, one finds that the phenotypic distribution is strongly shifted toward the less severe end (Figure 2B)—in this example, 33% of the cuticles fall in the least severe classes (embryos to the left of the dotted line in Figure 2B). On the basis of this, we focused on the frequency of embryos in the least severe classes. To score whether a Deficiency suppressed the arm^{XP33} phenotype, we prepared cuticles from the dead embryos, scored their phenotypes, and calculated the percentage of cuticles in the least severe classes; if this was at least six times the frequency in the control (*i.e.*, ≥3%), we scored this as an interaction.

By these criteria, 32 deficiencies interacted with arm^{XP33} (Table 1); a representative suppressed cuticle is shown in Figure 3B. Tables 1 and 2, Figure 4, and appendixes a and b summarize the screen, showing which regions were covered by deficiencies and which regions interacted. In all cases the suppression was qualitatively similar; embryos in the least severe class showed an increase in cuticle length, improvement in dorsal closure, and an increase in denticle diversity. The fraction of cuticles in the least severe phenotypic class ranged from 3 to 40% (each number is an average of two to three independent crosses; Tables 1 and 2). We retested each interacting stock—all reliably interacted although in some cases the percentage of suppression varied. Of the 32 stocks that interacted, we arbitrarily made a cutoff between "weak" and "strong" interactions at the level of 6% of the embryos in the least severe phenotypic classes. Eighteen Deficiencies were thus classified as weak interactors, with 3–5.9% of the cuticles in the least severe category (Table 1; appendixes a and b). Although this degree of suppression was reproducible, there were enough regions that suppressed arm^{XP33} more robustly that weakly interacting regions were not investigated further. We noted in passing that six stocks had hemizygous dominant cuticle phenotypes other than effects on segment polarity (Table 2B); one was also one of the strong interactors.

TABLE 1

Summary of the Deficiency screen by chromosome

Chromosome	No. of stocks/chrom.	(0–2.9%) No interaction	(3–5.9%) Weak interaction	(>6%) Strong interaction
2	67	47	12	8
3	64	53	6	5
4	3	2	0	1
Total	134	102	18	14

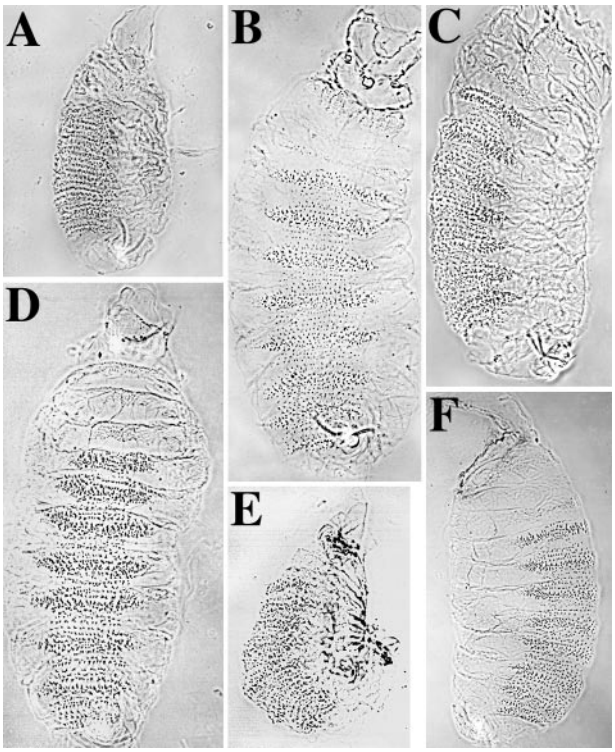

Figure 3.—Suppression by Deficiencies from the screen and *Dpresenilin*. (A) arm^{XP33}/Y. (B) arm^{XP33}/Y; *Df(2R)PC4*/+. Example of the suppression observed in the screen. (C) arm^{XP33}/Y; $Dpresenilin^{10}$/+. Heterozygosity for *Dpresenilin* significantly suppressed the arm^{XP33} phenotype. (D) Putative arm^{XP33}/Y; $Dpresenilin^{10}$/*Df(3L)ri-79c* embryo. A slightly more robust suppression was seen in progeny of flies heterozygous for $Dpresenilin^{10}$ crossed to flies heterozygous for *Df(3L)ri-79c*. (E) arm^{YD35}/Y. The zygotic null allele. (F) arm^{YD35}/Y; $Dpresenilin^{10}$/+. Heterozygosity for *Dpresenilin* also suppressed arm^{YD35}.

Fourteen deficiency stocks were "strong" interactors; with 6–40% of the cuticles in the least severe classes (Tables 1 and 2; Figure 4). Two of these deficiencies, *Df(3L)W10* and *Df(3L)Cat*, overlap, suggesting that the gene responsible for that interaction lay in the overlapping region (75B8;C1-2) and reducing the number of interacting genomic regions to 13. While two other interacting deficiencies, *Df(2L)spd* and *Df(2L)TE29*, should not quite overlap based on their reported cytology, they fail to complement one another, strongly suggesting that they do in fact overlap, reducing the number of interacting regions to 12. We analyzed other deficiencies in the regions of the strongly interacting Deficiencies, allowing us in most cases to further pinpoint the interacting region (see appendixes a and b for details). In four cases, smaller interacting Deficiencies were identified. In nine cases, overlap of the original deficiency with other Deficiencies that either interacted or did not interact allowed us to further define the interacting region.

None of the deficiencies tested resulted in any obvious enhancement of the arm^{XP33} phenotype, either producing defects in epithelial integrity or enhancing the segment polarity defects. The wild-type maternal contribution of Arm appears to completely provide adherens junction function, so reducing levels of components required for adherens junction function by 50% apparently does not affect epithelial integrity in arm^{XP33} mutants. In fact, when Müller and Wieschaus examined embryos homozygous for large deficiencies, they found no regions that were zygotically essential for adherens junction assembly and few that had a strong effect on junction function (Müller and Wieschaus 1996). We realized in retrospect that the severity of the arm^{XP33} segment polarity phenotype made it unlikely one could reliably recognize an enhancer of this defect.

One possible confounding factor was that mutations on the Balancer chromosomes with which the Deficiency chromosomes were heterozygous could have been the true cause of the phenotypic suppression. We think this is quite unlikely, as only a small number of Balancer chromosomes were used and none showed a consistent effect on the *arm* phenotype. A second potential problem is that second site mutations on the Deficiency chromosomes could in principle be responsible for certain observed interactions. This is highly unlikely for the seven strongly interacting regions that are defined by either two or more interacting Deficiencies or by a Deficiency and an identified gene (Figure 4). For the other five strongly interacting regions, some may be due to linked mutations outside the Deficiency interval, although given the overall frequency at which interactions were detected, we think this is unlikely to be the case for all.

Finding interactors by testing candidate genes: Our first approach to identify the gene(s) within each Deficiency responsible for the interaction was to test candidate genes in each region. We considered as candidate genes those with a mutant phenotype indicating an effect on cell fate choice in the ventral epidermis, genes known to act in Wg signaling, and genes known to affect cell-cell junctions or the actin cytoskeleton. We identified one interactor by this candidate gene approach and ruled out many other candidates by two methods: testing complementation between a candidate and the interacting deficiency and checking directly whether the candidate could suppress *arm*.

We tested four candidate genes that are part of the Wg signal transduction pathway or that affect segment polarity: *dTCF*, *cubitis interruptis*, *naked*, and *wg*. Removing one copy of the fourth chromosome gave a very strong interaction. In examining candidates on the fourth chromosome, we found that mutations in the gene encoding the DNA-binding protein dTCF, which is required for Wg signaling, suppress arm^{XP33}. This was a surprise and revealed a previously unexpected role for dTCF as a repressor as well as an activator of Wg-responsive genes (Cavallo *et al.* 1998). However, while null alleles of *dTCF* interact strongly, they do not suppress arm^{XP33} to the same degree as removing the entire

TABLE 2

Deficiencies that had a strong interaction with *arm^{XP33}*

A. Original interacting deficiency	Smallest region	% Supp.	Gene
Df(2L)sc19-5/SM6b, Cy[1] Roi[1]; Dp(2;1)B19, Df(1)y-ac, sc[1] pn[1], ed[1] dp[o2] cl[1]	25C8-9;25D2-4	7.9	
Df(2L)spd, al[1] dp[ov1]/CyO	28B3-4;28C	6.0	
In(1)w[m4h], y[1]; Df(2L) TE29Aa-11/CyO	28E4-7;29B2-C1	7.0	
Df(2L)TW137, cn[1] bw[1]/CyO, Dp(2;2) M(2) m[+]	36CD1-E1; 36E1-E2	6.6	
Df(2R)ST1, pr[1] cn[*]/CyO	42B3-5;42E	6.0	
Df(2R)PC4/CyO	55C;55F	9.5	
Df(2R)017/SM1	56F5;56F15	11.0	
Df(3L)W10, ru[1] h[1] Sb[sbd-2]/TM6b	75A6-7;75C1-2	14.0	*hid*
Df(3L)Cat, ri[*] e[*]/TM6	75B8;75F1	9.8	*hid*
Df(3L)Pc-MK/TM3, Sb[1] Ser[1]	78A2-78C9	7.0	
Df(3R)Scr, p[p] e[s]/TM3	84A1-2;84B1-2	9.3	
Df(3R)p712, red[1] e[1]/TM3	84D3-5;84F1-2	10.0	*puc*
Df(3R)D1-BX12, ss[1] e[4] ro[1]/TM6B	91F5;92D3-6	6.0	
C(4)RM, ci[1] ey[R]	101F1;102B	37.0	*dTCF*
B. Hemizygous dominant phenotype			
Df(3L)31A/Dp(3;3)C126, st[1] cp[1] in[1] ri[1] p[1]	78A;78E, 78D;79B		
Dp(3;1)2-2, w[1118]/?;Df(3R)2-2/TM3	81F;82F10-11;3D		
Df(3R)p712, red[1] e[1]/TM3	84D4-6;85B6, 25D;085B6		*puc*
Df(3R)P14, sr[1]/T(2;3)ap[Xa]	90C2-D1;91A1-2		
Df(3R)23D1, ry[506]/TM3 Sb[1]/mus309[Horka] e[1]	93F-94F1-6		
Df(3R)awd-KRB, ca[1]/TM3, y[+] Sb[1] e[1] Ser[1]	100C;100D		

A: Column 1, the original interacting Deficiencies from the Deficiency kits; column 2, the smallest interacting region, derived from comparing interacting and noninteracting Deficiencies (see appendixes a and b for details); column 3, the percent of individuals in the weakest phenotypic classes; column 4, identified interacting genes. B: Six Deficiencies were associated with partially penetrant dominant phenotypes. One also was a suppressor.

fourth chromosome. Thus, there may be a second suppressor on the fourth chromosome. *cubitis interruptis*, a gene involved in *hedgehog* signaling, was ruled out as this suppressor by testing a null allele for interaction (Cavallo *et al.* 1998). *naked* is a known negative regulator of Wg signaling and maps near *Df(3L)Cat*. However,

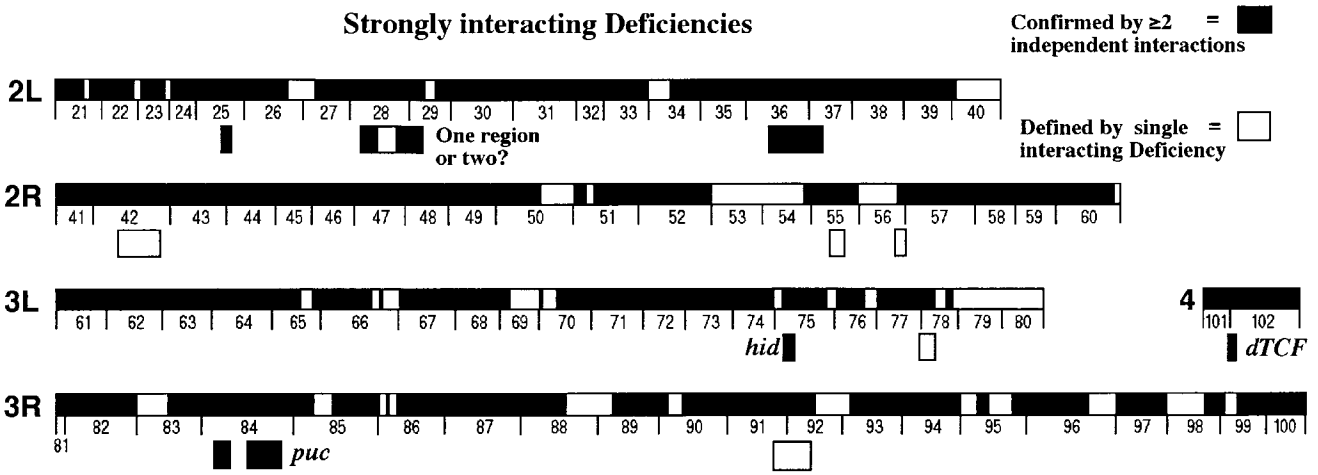

Figure 4.—Schematic summary of the screen. We estimate that ≥80% of the euchromatin of chromosomes 2, 3, and 4 were covered. Regions covered are represented by the black portions of the chromosomes; white portions are regions for which we were unable to find deficiencies. Black boxes below chromosomes represent regions containing putative suppressor(s) defined by the overlap between two or more deficiencies, or where an interacting gene was defined. White boxes represent regions defined by a single interacting Deficiency (see appendix for details).

it complemented this Deficiency and was thus ruled out. Two deficiencies, *Df(2L)TE29* and *Df(2L)spd*, are in the vicinity of *wg*. While *wg* is a positively acting component of the pathway, our experience with dTCF made us cautious in ruling it out without a test. We found that: (1) *wg* complements *Df(2L)TE29* and (2) a *wg* null does not suppress *arm*. This ruled *wg* out, although *DWnt4*, which maps near *wg* (Graba *et al.* 1995), remains a candidate. Finally, we tested alleles of two segment polarity genes that fell outside regions included in the Deficiencies in the kit: *hedgehog* and *teashirt*, which encodes a transcription factor that physically and functionally interacts with Arm (Gallet *et al.* 1998). Neither suppressed arm^{XP33}.

We also tested several genes with roles in cell-cell adhesion or cytoskeletal function. One was *DE-cadherin (shotgun)*, which we already knew could suppress *arm*. *Df(2)017* was suggested by its cytology to remove *DE-cadherin*, but both an allele of *DE-cadherin* and the small deficiency *Df(2)E2* that removes *DE-cadherin* (Uemura *et al.* 1996) complement *Df(2)017*. Thus this interaction is due to a different gene. Three other genes that regulate the cytoskeleton, *enabled* (*ena*; Gertler *et al.* 1995), *quail* (Mahajan-Miklos and Cooley 1994), and *scraps* (Schupbach and Wieschaus 1989), map to regions covered by interacting Deficiencies (56B5, 36C2-11, and 43E7, respectively). *ena* is an actin cytoskeleton regulator, *quail* encodes a vinculin-like protein thought to associate with actin, and *scraps* is required for the cytoskeletal events of cellularization. *ena* was included in interacting deficiency *Df(2R)PC4* by complementation (we did not test *quail* and *scraps* by complementation). However, when we tested alleles of all three genes, none suppressed arm^{XP33}. *18-wheeler*, a putative cell-adhesion molecule (Eldon *et al.* 1994) that maps in or near *Df(2R)017*, also did not suppress arm^{XP33}.

As a partial test of the effectiveness and completeness of the screen, we also tested a series of additional candidate genes, some of which fell outside Deficiencies in the kit and others of which were probably included in these Deficiencies but which we expected might physically or functionally interact with Arm. The vast majority did not show an interaction. We tested a variety of genes encoding components of other signal transduction pathways that pattern the dorsal or ventral epidermis: (1) the Hedgehog pathway, $hedgehog^{Ac}$; (2) the Dpp pathway, $decapentaplegic^{e87}$ and $screw^{J1}$; (3) the EGF receptor (EGFR) and other receptor tyrosine kinase pathways, $spitz^{2A14}$, $vein^{147\text{-}2}$, $argos^{257}$, $Egfr^{C18}$, $ras85D^{e1B}$, $rolled^{C18}$, $yan^{XE\text{-}12}$, and $torso^{1}$; and (4) the Jun N-terminal kinase pathway, *basket* and $Djun^{1}$. Of these, only $spitz^{2A14}$ interacted, and even in this case, only 3.8% fell into the weakest phenotypic categories, just above our cutoff for a weak interaction. We also tested five genes affecting the cytoskeleton or cuticle integrity: $krotzkopf\ verkehrt^{1}$, $myoblast\ city^{C1}$, $shroud^{1}$, $steamer\ duck^{3R\text{-}17}$, and $scraps^{8}$. None interacted. Finally, we tested one candidate among proteins that interact with mammalian β-catenin but for which the function of this interaction is not known. This was *Drosophila presenilin*, homolog of the mammalian presenilin family of transmembrane proteins (reviewed in Haass and De Strooper 1999). Mammalian Presenilins bind mammalian β-catenin (Zhou *et al.* 1997; Murayama *et al.* 1998; Yu *et al.* 1998; Levesque *et al.* 1999). Further, misexpression and other experiments suggest that mammalian Presenilins may regulate Wnt signaling (Murayama *et al.* 1998; Zhang *et al.* 1998; Kang *et al.* 1999; Nishimura *et al.* 1999a). In contrast to the other candidates tested, *D. presenilin* showed a very strong interaction. Heterozygosity for *D-presenilin* strongly suppressed arm^{XP33} (14.6% with weakest phenotypes; Figure 3, A *vs.* C) and also suppressed the zygotic null *arm* allele, arm^{YD35} (Figure 3, E *vs. F*). A surprise from these results was that although *Dpresenilin* was removed by two of the Deficiencies tested, *Df(3L)ri-79c* and *Df(3L)rdgC-co2*, neither showed a significant interaction (percentage of suppressions = 1.8 and 1.5%, respectively). This suggests that some interactions are sensitive to genetic background, and thus not all potential haplo-insufficient interactors were identified in our screen.

***P*-element lethals that interacted:** Our second approach to identifying genes responsible for an interaction was to use the collection of *P*-element-induced lethal mutations (hereafter called *P*-lethals) characterized by the Berkeley Drosophila Genome Project. These lethals are caused by *P*-element transposon insertions and are thus molecularly tagged, facilitating cloning. The available *P*-lethals are estimated to hit ~25% of essential genes (Spradling *et al.* 1999). One caveat to using these mutations to uncover a dose-sensitive suppressor is that there is no guarantee that the *P*-lethal will be a null allele, as is a Deficiency. *P*-transposons tend to insert either in the 5′ untranslated region or in introns, thus creating mutations that often are not null in phenotype and thus do not, when heterozygous, reduce gene function by 50%.

We obtained the *P*-lethals available from the Bloomington Stock Center (81 stocks) and the Kiss collection (73 stocks) in each of the interacting regions and tested their ability to suppress arm^{XP33}. A list of the *P*-lethal stocks tested is in a data supplement at http://www.genetics.org/cgi/content/full/155/4/1725/DC1. Of the *P*-lethals tested, we found two that suppressed arm^{XP33}. One of these, *l(3)A251.1*, mapped to region 84E. By examination of its homozygous phenotype and subsequent complementation tests, we learned that this is an allele of *puckered* (Martin-Blanco *et al.* 1998). A detailed examination of the biology underlying this interaction is presented in McEwen *et al.* (2000).

The apoptosis-promoting gene *head involution defective* is a dose-sensitive suppressor of *arm*: The second *P*-lethal that interacted with *arm* was *l(3)05014*, which maps to 75C1-2 and gave as strong a suppression as either of the interacting deficiencies in this region.

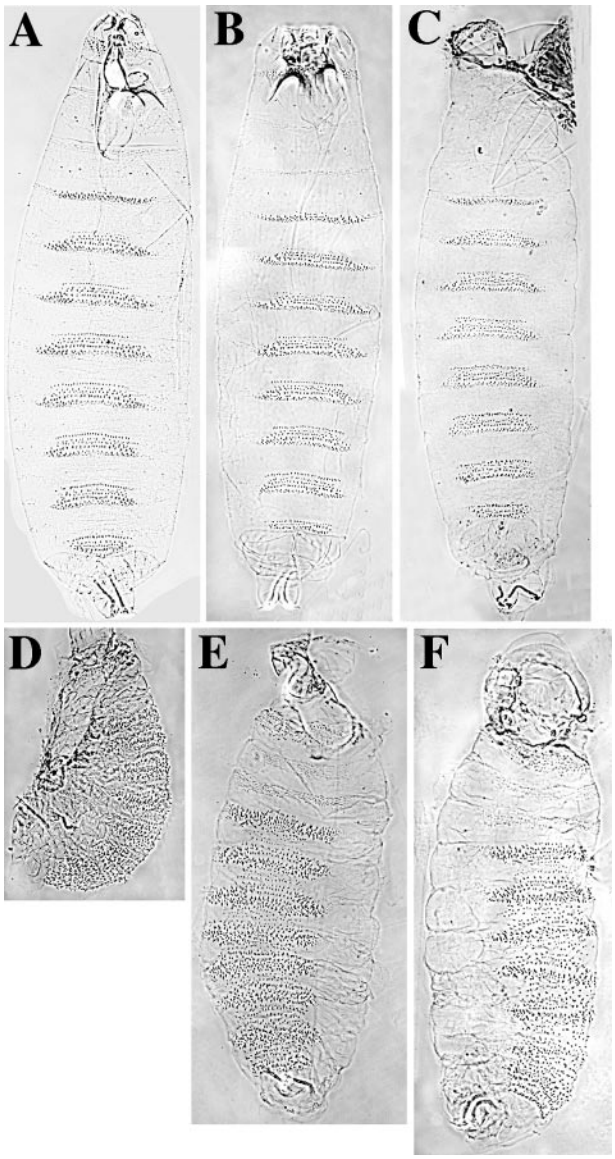

Figure 5.—Decreasing cell death suppresses *arm*. Wild type (A), hid^{05014} homozygotes (B), and *Df(3L)H99* homozygotes (C) have very similar cuticle phenotypes. hid^{05014} and *Df(3L)H99* homozygotes have head defects, but their segment polarity is normal. (D) arm^{XP33}/Y (E) arm^{XP33}/Y; hid^{05014}/+. Removing one copy of *hid* suppresses arm^{XP33}. (F) arm^{XP33}/Y; *armGAL4/UAS-p35*. Expression of the baculovirus antiapoptotic protein p35 in an arm^{XP33} mutant background also suppresses *arm*.

l(3)05014 is an allele of *head involution defective* (Grether *et al.* 1995). This allele is likely to be a null, as the *P*-element is inserted early in the protein-coding region. Null mutations in *hid* are embryonic lethal with defects in head involution during embryonic development (Abbott and Lengyel 1991; Figure 5, A *vs.* B), although occasional escapers survive to adulthood. More recently, it was revealed that *hid* mutations affect programmed cell death.

The machinery that triggers PCD in Drosophila has been the subject of intense investigation (reviewed in Abrams 1999). This work was initiated by a screen for genomic regions required for PCD (White *et al.* 1994). When chromosomal region 75C1-2 is deleted, in embryos homozygous for the small deficiency *Df(3)H99*, essentially all PCD in the embryo is eliminated (White *et al.* 1994). Subsequent analysis revealed that this chromosomal region contains three genes involved in PCD: *hid*, *reaper*, and *grim* (reviewed in Abrams 1999). Ectopic expression of any of these will trigger PCD. However, loss-of-function mutations are only available for *hid*. In *hid* mutants, a subset of the cells that normally undergo PCD do not do so (Grether *et al.* 1995), resulting in defects in head development. In embryos homozygous for *Df(3L)H99*, which thus lack *hid*, *reaper*, and *grim*, all PCD is abolished (White *et al.* 1994); these embryos have slightly stronger defects in head development (Figure 5C).

hid plays an important role in PCD. Ectopic expression of *hid* is sufficient to induce PCD in the eye, and this is completely suppressed by the baculovirus caspase inhibitor p35, suggesting *hid* acts upstream of caspases (Grether *et al.* 1995). *hid* has no clear homologs in other organisms; however, Hid overexpression triggers PCD in mammalian cells. Hid, Reaper, and Grim all share a short region of weak sequence similarity near their N termini. In Hid, this region is required for initiating cell death in mammalian tissue culture, while Hid's C terminus is required for localization to mitochondria, an organelle involved in PCD (Haining *et al.* 1999). Recent work supports the idea that Hid functions by blocking interaction between Inhibitor-of-apoptosis (IAP) family caspase inhibitors and caspases (Vucic *et al.* 1998; Wang *et al.* 1999).

Heterozygosity for hid^{05014} suppresses arm^{XP33} (Figure 5, D *vs.* E), as well as the zygotic null allele arm^{YD35} (data not shown). Heterozygosity for an X-ray-induced loss-of-function allele, hid^{WR+X1}, causes the same degree of suppression, further supporting the idea that *hid* is the gene responsible for the interaction. In addition, we generated revertants of the *P* element in hid^{05014} by mobilizing the *P* element and screening for viable stocks that lost the genetic marker carried by the *P* element. These revertant chromosomes fail to suppress arm^{XP33} (data not shown). Further reducing *hid* levels by making embryos homozygous for hid^{05014} does not increase the degree of suppression of arm^{XP33}. Likewise, either heterozygosity or homozygosity for the small deficiency *Df(3L)H99*, which removes *hid*, *grim*, and *reaper*, suppresses arm^{XP33} to the same degree as removal of one copy of *hid*.

The suppression by *hid* can be mimicked by blocking PCD: PCD is elevated in segment polarity mutants (Martinez Arias 1985; Klingensmith *et al.* 1989; Pazdera *et al.* 1998). The dramatically shortened cuticle secreted by an *arm* mutant is presumably caused, at least in part, by loss of ventral epidermal cells via PCD. The suppression of arm^{XP33} by hid^{05014} could thus be due to Hid's role in PCD; alternately, it could be due to an unknown

function of Hid. To test if the *arm* suppression results from an effect on PCD, we reduced embryonic PCD by expressing the baculovirus antiapoptotic protein p35, which acts as a caspase inhibitor; p35 suppresses the PCD triggered by *hid* overexpression in the fly eye (Grether *et al.* 1995). We found that arm^{XP33} mutant embryos in which we ubiquitously expressed p35 using the GAL4-UAS system (Brand and Perrimon 1993) had a suppressed phenotype (Figure 5, F *vs.* D). The suppression by p35 was similar in degree to that resulting from *hid* heterozygosity (Figure 5E). This suggests that decreased PCD in the embryo can suppress *arm* and supported the idea that the interaction between *hid* and *arm* was due to *hid*'s role in PCD.

***hid* suppresses *wg* in a highly dose-sensitive fashion:** We next tested whether the effect was *arm* specific or whether reduction in PCD would suppress the phenotype caused by other reductions in Wg signaling. To do so, we examined whether reduction in PCD suppressed a null allele of *wg*, wg^{IG22}. wg^{IG22} mutant cuticles have a lawn of uniform, large denticles covering the ventral epidermis (Nüsslein-Volhard and Wieschaus 1980; Figure 6A), and they are much smaller than wild type, but unlike *arm* mutant cuticles they are usually closed dorsally. We tested whether heterozygosity or homozygosity for either *hid* or for *Df(3L)H99* suppressed wg^{IG22}.

hid modified wg^{IG22} in a dose-sensitive fashion, but the nature of the phenotypic modification was different from that seen with *arm*. There was not any pronounced improvement in the *wg* segment polarity defect; in wg^{IG22}; hid^{05014} (Figure 6B) or wg^{IG22}; *Df(3L)H99* (Figure 6C) double mutants, all cells still secrete a uniform lawn of denticles, and the cuticle of the wg^{IG22}; *Df(3L)H99* double mutant remains much smaller than that secreted by a wild-type embryo, contrasting with the increase in cuticle size in *arm; Df(3L)H99* double mutants. However, we found a striking effect of *hid* dose on the number and size of the denticles on the ventral epidermis. The number of denticles is more than doubled in wg^{IG22}; *Df(3L)H99* compared to wg^{IG22} alone, and the denticles secreted by the double mutant are much smaller than those in the *wg* null (Figure 6, A *vs.* B and C; the change in denticle size may be less meaningful, as denticle size is also somewhat reduced in *Df(3L)H99* homozygotes that are wild type for *arm* and *wg*; Figure 5C).

wg^{IG22} is less sensitive to reduction in *hid* dose than *arm*, and thus the effect on wg^{IG22} is additive. Removal of one copy of *hid* in a wg^{IG22} background has only a subtle effect on cuticle pattern (data not shown), while removal of both copies of *hid* has a stronger effect (Figure 6, B *vs.* A). Removing one copy of the region covered by *Df(3L)H99* has a greater effect than removing both copies of *hid* (data not shown), suggesting that removing all three cell death genes results in a more pronounced interaction. The effect on cuticle pattern is thus most pronounced in wg^{IG22}; *Df(3L)H99* double mutants (Figure 6C), which have many more, much smaller denticles than does a wg^{IG22} single mutant (Figure 6A). To confirm this, we labeled embryos with phalloidin to visualize the filamentous actin in denticles and with TUNEL to identify embryos with cells undergoing PCD. Embryos homozygous for *Df(3L)H99* do not label with TUNEL, as they have no PCD, allowing us to unambiguously identify double mutants. The results matched the cuticle data: wg^{IG22} mutants showed the characteristic lawn of denticles (Figure 6F), while wg^{IG22}; *Df(3L)H99* double mutants (embryos without cells undergoing PCD as measured by TUNEL) had many more much smaller denticles (Figure 6E). In the course of this analysis, we also observed that *Df(3L)H99* mutants have significantly more epidermal tissue in the head (as was previously observed by Grether *et al.* 1995) and in the lateral epidermis (Figure 6, J *vs.* K), consistent with the idea that wild-type embryos reduce the number of epidermal cells via PCD. We also examined whether reduction in PCD suppressed a weaker *wg* heteroallelic combination, wg^{PE4} / *Df(2)DE*. We saw no noticeable suppression of the segment polarity phenotype and no noticeable increase in denticle number caused by either heterozygosity or homozygosity for *Df(3L)H99* (data not shown). This may not be surprising as this weaker *wg* phenotype likely primarily reflects changes in cell fate without significant ectopic cell death, as the cuticle is nearly wild type in length.

Blocking cell death in wg^{IG22} increases cell number but decreases cell size: The novel phenotype of wg^{IG22}; *Df(3L)H99* double mutants could have several causes. Extra denticles could result if individual cells secreted more denticles; alternately, they could result from an increased number of cells. To distinguish these possibilities, we examined the cell morphology of wild type, wg^{IG22}, and wg^{IG22}; *Df(3L)H99* double-mutant embryos, using antibodies to phosphotyrosine to outline ventral epidermal cells and to label developing denticles. In wild-type embryos (Figure 6G), ventral epidermal cells form a reiterated pattern of denticle-secreting cells, which are very narrow in the anterior / posterior (A / P) axis, and naked cuticle-secreting cells, which are much less narrow. There are, on average, 12 rows of cells per segment. In contrast, in *wg* mutants there are only 8 rows of cells per segment (Figure 6H; the segment boundary was determined by comparison of the denticle pattern in cuticles to the phosphotyrosine pattern). In the wg^{IG22}; *Df(3L)H99* double mutant, cell number is greatly increased relative to the wg^{IG22} single mutant. The double mutant has 12 to 14 rows of cells (Figure 6I), equaling or exceeding the number of cell rows in the wild type. Thus eliminating PCD in a wg^{IG22} mutant embryo increases cell number, as expected.

Blocking cell death in a wg^{IG22} mutant also had a second, unexpected consequence—cell size was significantly decreased. As mentioned above, in wild-type embryos anterior denticle-secreting cells are narrowed in the A / P axis, while posterior naked cuticle-secreting

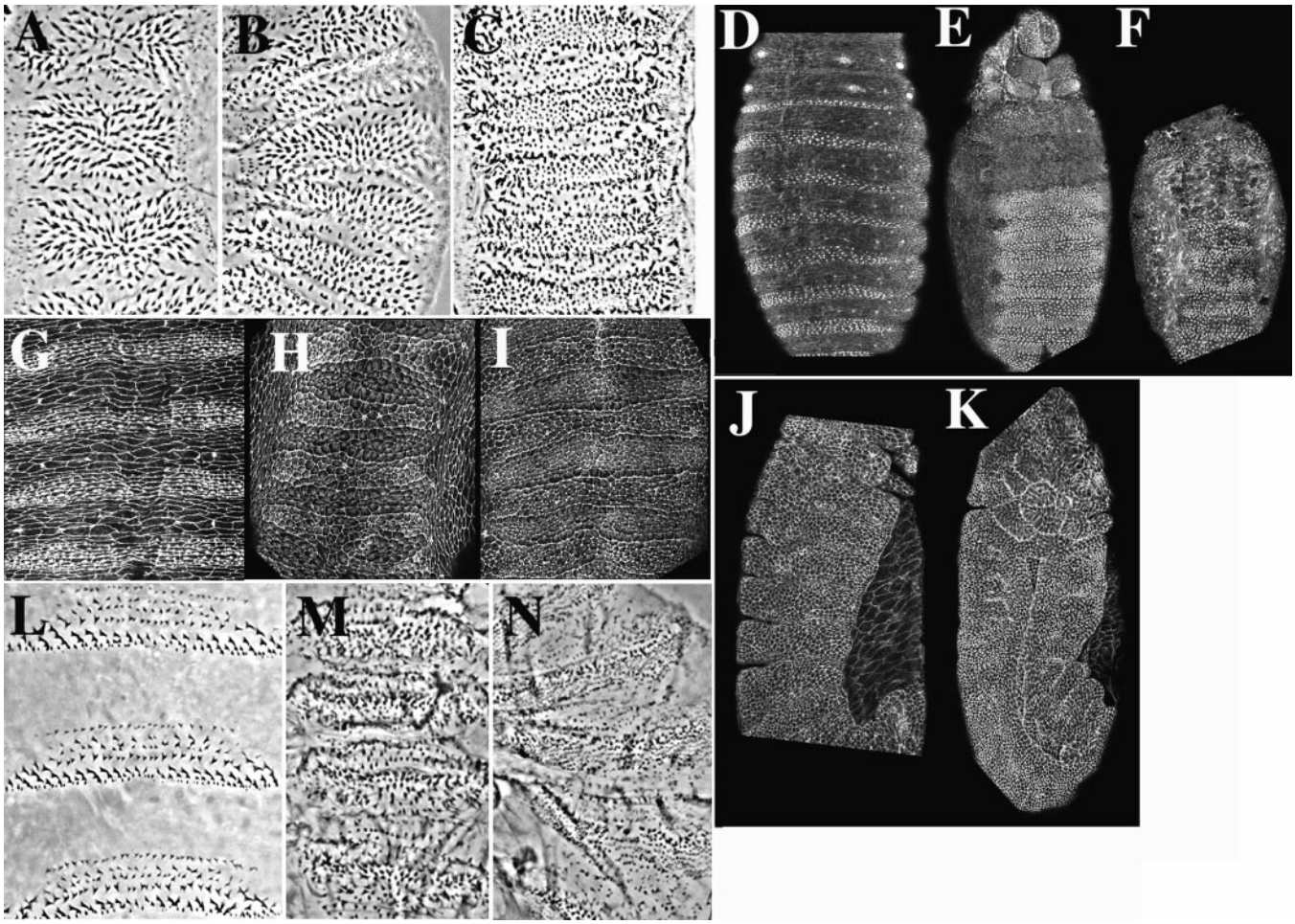

Figure 6.—Reducing PCD suppresses *wg* in a dose-sensitive fashion. (A–C) Cuticle preps. (D–F) Embryos labeled with phalloidin, which recognizes f-actin and thus highlights denticles. These embryos were also labeled via TUNEL (data not shown) to confirm their genotypes. (A, F) *wg* null mutants completely lack segment polarity and have only large, thick denticles. (B) wg^{IG22}; hid^{0501}. (C, E) wg^{IG22}; *Df(3L)H99*. (D) Wild type. In the double mutants, denticle number greatly increases. (G–K) Embryos stained with antiphosphotyrosine antibody to outline cells. (G) Wild type, showing reiterated groups of narrow cells, which will secrete denticles, and less narrow cells, which will secrete naked cuticle. There are 12 rows of cells per segment. (H) *wg* single mutants have fewer, larger cells. All cells are cuboidal, and there are about 8 rows of cells per segment. (I) *wg; Df(3L)H99* double mutants have many more ventral epidermal cells than *wg* single mutants—there are 12 to 14 rows of cells per segment. Cells in the double mutant are much smaller. (J) Lateral view of a wild-type embryo during germband retraction. (K) *Df(3L)H99* at the same stage, revealing an increased number of cells compared to wild type. Excess cells form a lateral fold and ectopic folds near the maxillary and labial segments and toward the posterior. (L) Wild-type cuticle. (M) arm^{XP33}. (N) arm^{XP33}; *UAS-dsh/VP16::armGAL4*. Expressing high levels of *dsh* in arm^{XP33} results in an increase in denticle number and reduction in denticle size, similar to that in *wg; Df(3L)H99* double mutants.

cells are not. In contrast, in a *wg* mutant all cells are both uniformly cuboidal (Figure 6H) and significantly larger than denticle-producing cells of a wild-type embryo. This increase in size likely reflects an increase in cell volume, because in optical cross sections wg^{IG22} and wild-type cells were the same height (data not shown). In contrast, cells of wg^{IG22}; *Df(3L)H99* double mutants are much smaller than those in *wg* single mutants (Figure 6I). Ventral cells of double mutants do resemble wg^{IG22} single mutants in several ways; most cells are cuboidal, the cells create a pattern of block-like pseudosegments (though with more rows of cells than in *wg* single mutants), and all cells secrete denticles. We do not have a good explanation for the qualitative difference in the effect of *hid* on the *arm* and wg^{IG22} phenotypes. We observed one other situation where manipulating Wg signaling resulted in an increased number of smaller denticles. Overexpression of *dsh* using the GAL4-UAS system in an arm^{XP33} mutant gives rise to a cuticle with many very small denticles, but with the length of an arm^{XP33} single mutant (Figure 6, M *vs.* N). Dsh is a positive effector of Wg signaling mapping upstream of Arm in the Wg pathway; we imagine that Dsh overexpression slightly augments the residual Wg signaling in an *arm* zygotic mutant.

Our comparison of wg^{IG22} and wg^{IG22}; *hid* suggests that

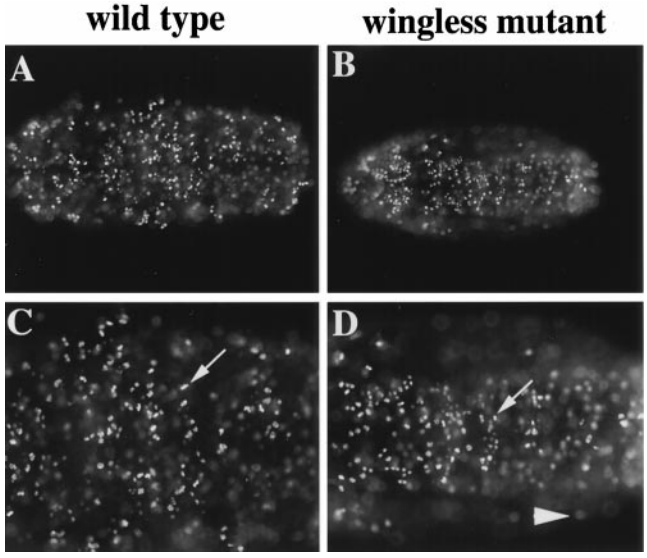

Figure 7.—*wg* mutants enter mitosis 16 in the ventral epidermis. Ventral views of representative wg^{IG22} (B, D) and phenotypically wild-type sibling (A, C) embryos stained with antiphosphohistone H3 antibodies. The magnification in C and D is twice that of A and B. Arrows in C and D indicate condensed chromosomes of cells that were counted. Only mitotic figures in the epidermis were included in the counts; out of focus staining (*e.g.*, arrowhead) is from mitotic cells in the underlying central nervous system. Embryos were from a wg^{IG22}/*CyO ftz-lacZ* stock, allowing unambiguous identification of *wg* mutants by lack of β-galactosidase expression. *wg* mutants were also apparent due to defects in the normal segmental pattern of S phase and mitosis.

an increase in PCD contributes to the reduced number of ventral epidermal cells in *wg*, consistent with previous observations (Pazdera *et al.* 1998). This might also explain the increased cell size in *wg* mutants, as epidermal cells have been observed engulfing dying neighbors (Pazdera *et al.* 1998), thus potentially increasing their size. However, since Wnts are mitogens in certain cell types (*e.g.*, Dickinson *et al.* 1994; Neumann and Cohen 1996), we also considered an alternate explanation that could explain both reduction in cell number and increase in cell size in wg^{IG22} mutants: a failure to complete the normal program of cell division. Since no growth occurs within the embryo, as cells divide they are reduced in size, and thus if wg^{IG22} mutant cells failed to complete one round of mitosis, they would be twice as large.

We thus assessed the pattern of cell division in wg^{IG22}. Ventral epidermal cells divide three times after the blastoderm stage and arrest in G1 of the 17th embryonic cell cycle (Edgar and O'Farrell 1989). Cell divisions can be visualized by pulse labeling with BrdU to detect replicating nuclei or with an antibody that specifically recognizes a phosphoisoform of histone H3 that only occurs during mitosis (Figure 7; Su *et al.* 1998). Condensed mitotic chromosomes can be easily identified in fixed tissues with this antibody (Figure 7, C and D). We analyzed embryos at a time (stage 12) when cells of the ventral epidermis normally complete their 16th cell cycle, to see if wg^{IG22} mutants fail to undergo this last cell division. BrdU labeling indicated that ventral epidermal cells replicate during S phase 16 in wg^{IG22} mutants (data not shown). In addition, mitotic figures are as readily apparent in the ventral epidermis of stage 12 wg^{IG22} mutant embryos as they are in wild type (Figure 7, A and B). Thus, lack of Wg activity does not cause inappropriate cell cycle arrest. To compare the mitotic index between wild type and wg^{IG22}, we counted the total number of phosphohistone H3 positive nuclei of the ventral surface of individual embryos (arrow in Figure 7, C and D). There was no significant difference between the average number of mitotic cells in wild-type (175 ± 75.7; $n = 7$) *vs.* wg^{IG22} mutant (232 ± 44.2; $n = 9$) embryos. The variance in the absolute numbers of mitotic cells from embryo to embryo can be attributed to at least two factors: First, the precise age of each embryo scored differs slightly, as stage 12 spans ~2.5 hr of development at 25°, and second, there is some cell cycle asynchrony among individual cells of a particular epidermal region that enter mitosis "together" (*i.e.*, mitotic domains). We conclude that wg^{IG22} mutant embryos complete the normal number of cell divisions in the ventral epidermis, supporting the idea that the reduction in cell number in this region of late stage wg^{IG22} embryos is primarily a consequence of elevated levels of PCD.

DISCUSSION

Drosophila Arm and its human homolog βcat are multifunctional proteins that play roles in cell-cell adherens junctions and in the transduction of Wg/Wnt signals. In both roles, Arm/βcat acts as a scaffold upon which a multiprotein complex is assembled. In addition to these well-documented roles, Arm/βcat associates with other proteins, such as the EGF receptor (Hoschuetzky *et al.* 1994), fascin (Tao *et al.* 1996), and Presenilin 1 (Zhou *et al.* 1997). The biochemical function of these complexes is unknown.

We desire to learn more about the known roles of Arm in adherens junctions and in Wg signaling and also to begin to learn what Arm might do with its other partners. Genetics offers the opportunity to look for proteins that are functionally linked with Arm without assumptions as to their identity or biochemical role. Our initial goal in the screen was to identify novel proteins essential for adherens junction assembly or structure. However, as in all genetic screens, we had cast our net much wider. In the four cases where we proceeded from Deficiency to single gene, none encode new junctional proteins and each reveals a separate aspect of Arm biology. The fourth chromosome interactor dTCF revealed a previously unexpected role for a known component of the Wg pathway, providing evidence that dTCF not only activates Wg responsive genes but also, in the ab-

sence of Arm, represses them (Cavallo *et al.* 1998). Characterization of the interactor in 84E, Puckered, revealed a novel role for a known protein and led to data suggesting that the JNK and Arm pathways act in parallel both in dorsal closure and in ventral patterning (McEwen *et al.* 2000). The interaction with Dpresenilin suggests that the biochemical interaction observed in mammalian cells has impact on Arm function *in vivo.* The fourth interactor, Hid, demonstrated that altering a downstream consequence of the loss of Wg signaling, programmed cell death, could suppress *arm* and, as is discussed below, suggested that Wg may act as a survival factor by modulating Hid activity.

We were initially concerned about the amount of labor required to screen for suppressors reducing the severity of an embryonic lethal phenotype without restoring viability (we expected that suppression to viability was unlikely). In retrospect, the screen, while labor intensive, was quite straightforward and could be applied to other embryonic lethal genes with a clear cuticle phenotype (*arm*'s position on the X chromosome eased the effort). Use of the Deficiency kit reduced the number of stocks screened, although having completed the screen we now believe one could carry out such a screen using individual mutagenized lines. Others also recently screened for suppressors or enhancers of embryonic lethal phenotypes, suggesting that this approach may be widely applicable (Raftery *et al.* 1995; Hudson *et al.* 1998; A. Bejsovec, personal communication).

Our screen had several limitations that affected the spectrum of genes identified. First, for a gene to be identified, it had to affect the *arm* phenotype in a dose-sensitive way. Second, the effect on *arm* had to be consistent and substantial. Our arbitrary cutoff for degree of interaction likely eliminated genes in the desired categories in which mutations did not sufficiently suppress *arm.* For example, loss-of-function mutations of Drosophila *abelson* or Deficiencies that remove it suppress *arm*, but not to a sufficient degree to be scored positive in our screen (Loureiro and Peifer 1998). Third, due to the allele of *arm* we chose, we could not reliably score enhancement of the segment polarity phenotype, and likewise, potentially due to high levels of maternal Arm, we did not detect any interactor that produced defects in epithelial integrity. Fourth, since many *P*-element alleles are not null, our ability to move from Deficiency to single gene using these mutations was consequently limited. Finally, genetic background may obscure some interactions—for example, we saw a clear genetic interaction with two alleles of *Dpresenilin* but saw no significant interaction with two Deficiencies that remove it.

During preparation of this manuscript, an article appeared describing a different strategy for identifying genetic interactors with *arm*, which provides an interesting comparison. Greaves *et al.* (1999) expressed in the posterior compartment of the wing the intracellular domain of DE-cadherin, which they previously found could sequester Arm and thus block its signaling activity (Sanson *et al.* 1996). In parallel they overexpressed Arm in the same place. Each caused a reproducible wing phenotype, which appears to reflect reduction and elevation of Wg signaling, respectively. They then screened for modifiers of these phenotypes using, as we did, the Deficiency kit. Many of the deficiencies tested thus overlapped (though not all, as we did not test the X chromosome and they did not test the fourth chromosome).

We compared the spectrum of modifying Deficiencies obtained in our screen with the 59 interacting Deficiencies identified in their screen. The Deficiencies identified were quite different, likely reflecting the distinct methods used to examine interaction and the different tissues involved. These differences illustrate the benefit of taking a variety of genetic approaches to modifier screens and emphasize that no one screen will identify all or even most potential interactors. Most interacting Deficiencies identified in their screen did not interact in our screen; for 39 of their interacting deficiencies, the percentage of suppression in our screen was $<3\%$. Eight of their interacting Deficiencies were weak interactors in our screen [*Df(2L)sc19-8*, *Df(2L)prd1.7*, *Df(2L)J32*, *Df(2L)H20*, *Df(3L)vin5*, *Df(3L)ZN47*, *Df(3R)crb87-5*, and *Df(3R)Hu*]. Four interacting Deficiencies from their screen, *Df(3L)Spd*, *Df(3L)Cat*, *Df(3R)D1-BX12*, and *Df(3R)p712*, were strong interactors in our screen. Within two of these latter regions we identified interactors: *hid* from *Df(3L)Cat* and *puc* from *Df(3R)p712.*

Even in cases where the two screens identified the same Deficiency, it is not clear that the same gene is responsible. First, in several cases different subsets of overlapping Deficiencies interacted in the two screens. Second, Greaves *et al.* (1999) identified interacting genes in many of their Deficiencies. In four cases, we also examined those candidates. Two were identified as interactors in our screen as well (*DE-cadherin* and *zw3*, used in our reconstruction experiments). In contrast, one of their interactors, *wg*, did not interact in our screen, even though a Deficiency that removes it, *Df(3L)Spd*, did interact. Likewise, components of the EGFR pathway interacted in their tests but not ours. Finally, in our hands *naked* complements *Df(3L)Cat*, thus ruling it out as our interactor in that region; in this region we identified *hid* as the interactor.

Hid activity, PCD, and the segment polarity phenotype: It has been known for more than a decade that PCD plays an important role in the segment polarity phenotype resulting from inactivation of either the Hedgehog or Wg pathways (Martinez-Arias 1985; Klingensmith *et al.* 1989). Recently, Minden and colleagues carried out a detailed analysis of this process, quantitating cell death in *wg*, *arm*, *gooseberry*, and *naked.* They found that the elevation in cell death affected particular cells (Pazdera *et al.* 1998). Since the first reports of cell death in segment polarity mutants, the

machinery that drives PCD in embryos has begun to be identified. Homozygosity for the small chromosomal Deficiency, *Df(3L)H99*, blocks essentially all PCD (White *et al.* 1994). Within this interval, three genes play roles in PCD: *grim*, *reaper*, and *hid* (reviewed in Abrams 1999). Ectopic expression of any of these can trigger PCD, but loss-of-function mutations are only available for *hid*.

Given the role of PCD in the segment polarity phenotype, it is perhaps not surprising that elimination of PCD would alter it. Several aspects of the effect of PCD reduction were unexpected, however. First, and most striking, the phenotypes of *arm* and *wg* mutants were very sensitive to relatively small changes in the dose of *hid* and the other cell-death promoters. For example, while heterozygosity for *hid* has no known effects on normal development, it strongly suppresses *arm*. Further reductions in the levels of *hid* or the other cell-death regulators had no additional effect on *arm*, suggesting that reducing the Hid dose by half eliminated the relevant ectopic PCD that occurs in an *arm* mutant. The *wg* phenotype was also suppressed in a highly dose-sensitive fashion, but in a different dosage range. A 50% reduction of *hid* caused slight but detectable effects, a 50% reduction in all three death promoters caused greater suppression, while homozygosity for the deletion removing all three genes resulted in the strongest *wg* suppression.

Recent observations regarding the role of Hid in PCD in the eye may explain this. Signaling through the ras/mitogen-activated protein kinase (MAPK) pathway promotes cell survival by antagonizing Hid (Bergmann *et al.* 1998; Kurada and White 1998). These authors suggested that Hid serves as a rheostat, with its levels determining the probability of PCD. They further suggest that Hid activity has to exceed a threshold to trigger PCD; the accumulation of *hid* mRNA in cells that are not programmed to die is consistent with this (Grether *et al.* 1995). Our observations further support this model. Wg signaling may normally antagonize Hid, potentially by regulating its expression. In embryos where Wg signaling is attenuated, elevated Hid activity may trigger PCD when it rises above a critical threshold. A threshold model could explain why the segment polarity phenotype is so sensitive to the dose of Hid and its partners.

Another surprise was the qualitative difference in the effect of cell death reduction on *wg* and *arm* mutants. While the resulting cell number was likely increased in both double-mutant genotypes in the *arm; hid* double mutant, the reduction in PCD restored an almost wild-type-length cuticle, while in the *wg; hid* double mutant, the increase in cell number was not reflected in an increase in cuticle length. The reason for this remains mysterious. One possible explanation for this discrepancy is the difference in the degree to which Wg signal is compromised in the two situations and the embryonic stage at which this disruption occurs. In the *wg* null, Wg signaling is totally eliminated from the beginning of development. In contrast, perdurance of maternal Arm substantially rescues early defects in Wg signaling in *arm* zygotic nulls (Klingensmith *et al.* 1989). *arm* mutants remain more normal in morphology than *wg* mutants through the onset of germband retraction and retain remnant denticle diversity. Thus when one eliminates PCD in an *arm* mutant a more normal pattern is restored. The difference in amount and timing of Wg signaling in the two backgrounds may also explain why *arm* mutants are affected by smaller alterations in Hid level. The remaining Wg signaling in an *arm* zygotic mutant may promote cell survival to some extent, meaning that a smaller reduction in Hid activity prevents ectopic PCD.

We were also surprised that reduction in cell death alleviated *arm*'s dorsal closure defect. We previously suspected that this defect was due solely to Arm's role as a catenin. However, recent data suggest that dorsal closure is promoted by Wg signaling (McEwen *et al.* 2000). We now suspect that defects in Wg signaling and catenin function combine to block dorsal closure in *arm* mutants. Restoring either rescues the *arm* dorsal closure defect. However, blocking PCD alone should not restore Wg signaling or catenin function. Perhaps the excess cell death in the head region or in the amnioserosa of an *arm* mutant contribute to its dorsal closure defect.

Presenilins and Arm function: While evaluating the effectiveness of our screen, we tested a variety of candidate genes, including some that mapped within noninteracting Deficiencies. Heterozygosity for one of these, *Dpresenilin*, strongly suppressed *arm*. Presenilins form a family of multipass transmembrane proteins that were first identified because missense mutations in two human Presenilins cause early onset familial Alzheimer disease (FAD; reviewed in Haass and De Strooper 1999; Nishimura *et al.* 1999b). The cell biological function of Presenilins and how dysfunction contributes to disease remain controversial. Genetic data in *Caenorhabditis elegans* and Drosophila implicate Presenilins in the function of Notch proteins, most likely via effects on protein processing. Likewise, human Presenilin mutations affect proteolytic processing of the plaque protein Aβ; this may lead to pathology (reviewed in Haass and De Stropper 1999). Recently, it was found that both βcat and other Arm repeat proteins such as δ-catenin associate with Presenilins *in vivo*. The function of this interaction remains confusing. Zhang *et al.* (1998) reported that wild-type Presenilin stabilizes βcat and that this is abrogated by missense mutations found in FAD patients, and Nishimura *et al.* (1999a) reported that *presenilin* missense mutant cells from FAD patients have less nuclear βcat. These data support a role for Presenilins as positive regulators of Wnt signaling via Arm/βcat. In contrast, both Muryama *et al.* (1998) and Kang *et al.* (1999) report that overexpression of wild-type Pre-

senilin destabilizes βcat; Kang *et al.* further show that βcat is stabilized in both *Presenilin1* null fibroblasts or if FAD mutants of *Presenilin1* are overexpressed, while Muryama *et al.* demonstrate that a Wnt-responsive promoter is downregulated by Presenilin overexpression. These data support a conclusion opposite from that above, in which wild-type Presenilins negatively regulate Wnt signaling. Finally, Georgakopoulos *et al.* (1999) suggest that the presenilin-βcat complex includes cadherins, in contravention of most other data. Our genetic data are most consistent with a model in which Presenilins negatively regulate Wg signaling (Figure 3) either directly or indirectly by binding Arm/βcat or by influencing adherens junction assembly. Clearly much work remains to differentiate between the different possible mechanisms.

We are very grateful to Clare Duffy, Tiernan Mennen, Joel Stein, Dave Roberts, and Christina Tuskey, who helped with the screen, to the Bloomington Drosophila Stock Center for patiently shipping and reshipping stocks, and to D. Curtis for providing the *Dpresenilin* alleles. We thank Susan Whitfield for her assistance with the figures. This work was supported by grants from the National Institutes of Health (NIH) to M.P. (GM-47857) and to R.J.D. (GM-57859). Work in the Duronio lab is also supported by the Cancer Research Fund of the Damon Runyon-Walter Winchell Foundation Award (DRS-10). R.T.C. was supported in part by NIH 5T32 GM-07092, D.G.M. and D.L.M. were supported in part by NIH 5T3 CA-09156 (D.G.M. and D.L.M.), National Research Service Award (NRSA) 1F32 GM19824 (D.G.M.), and NRSA 1F32 GM20019-01 (D.L.M.), and M.P. was supported in part by a Career Development Award from the U.S. Army Breast Cancer Research Program.

LITERATURE CITED

Abbott, M. K., and J. A. Lengyel, 1991 Embryonic head involution and rotation of male terminalia require the Drosophila locus *head involution defective*. Genetics **129:** 783–789.

Abrams, J. M., 1999 An emerging blueprint for apoptosis in *Drosophila*. Trends Cell Biol. **9:** 435–440.

Bergmann, A., J. Agapite, K. McCall and H. Steller, 1998 The Drosophila gene hid is a direct molecular target of Ras-dependent survival signaling. Cell **95:** 331–341.

Brand, A. H., and N. Perrimon, 1993 Targeted gene expression as a means of altering cell fates and generating dominant phenotypes. Development **118:** 401–415.

Cavallo, R. A., R. T. Cox, M. M. Moline, J. Roose, G. A. Polevoy *et al.*, 1998 *Drosophila* TCF and Groucho interact to repress Wingless signaling activity. Nature **395:** 604–608.

Cox, R. T., C. Kirkpatrick and M. Peifer, 1996 Armadillo is required for adherens junction assembly, cell polarity, and morphogenesis during *Drosophila* embryogenesis. J. Cell Biol. **134:** 133–148.

Dickinson, M. E., R. Krumlauf and A. P. McMahon, 1994 Evidence for a mitogenic effect of *Wnt-1* in the developing mammalian central nervous system. Development **120:** 1453–1471.

Edgar, B. A., and P. H. O'Farrell, 1989 Genetic control of cell division patterns in the *Drosophila* embryo. Cell **57:** 177–187.

Eldon, E., S. Kooyer, D. D'Evelyn, M. Duman, P. Lawinger *et al.*, 1994 The Drosophila 18 wheeler is required for morphogenesis and has striking similarities to Toll. Development **120:** 885–899.

Gallet, A., A. Erkner, B. Charroux, L. Fasano and S. Kerridge, 1998 Trunk-specific modulation of Wingless signaling in *Drosophila* by Teashirt binding to Armadillo. Curr. Biol. **8:** 893–902.

Georgakopoulos, A., P. Marambaud, S. Efthimiopoulos, J. Shioi, W. Cui *et al.*, 1999 Presenilin-1 forms complexes with the cadherin/catenin cell–cell adhesion system and is recruited to intercellular and synaptic contacts. Mol. Cell **4:** 893–902.

Gertler, F. B., A. R. Comer, J. Juang, S. M. Ahern, M. J. Clark *et al.*, 1995 *enabled*, a dosage-sensitive suppressor of mutations in the *Drosophila* Abl tyrosine kinase, encodes an Abl substrate with SH3 domain-binding properties. Genes Dev. **9:** 521–533.

Graba, Y., K. Gieseler, D. Aragnol, P. Laurenti, M. C. Mariol *et al.*, 1995 DWnt-4, a novel Drosophila Wnt gene acts downstream of homeotic complex genes in the visceral mesoderm. Development **121:** 209–218.

Greaves, S., B. Sanson, P. White and J.-P. Vincent, 1999 A screen for genes interacting with Armadillo, the Drosophila homolog of β-catenin. Genetics **153:** 1753–1766.

Grether, M. E., J. M. Abrams, J. Agapite, K. White and H. Steller, 1995 The *head involution defective* gene of *Drosophila melanogaster* functions in programmed cell death. Genes Dev. **9:** 1694–1708.

Haass, C., and B. De Strooper, 1999 The presenilins in Alzheimer's disease—proteolysis holds the key. Science **286:** 916–919.

Haining, W. N., C. Carboy-Newcomb, C. L. Wei and H. Steller, 1999 The proapoptotic function of Drosophila Hid is conserved in mammalian cells. Proc. Natl. Acad. Sci. USA **96:** 4936–4941.

Hay, B. A., T. Wolff and G. M. Rubin, 1994 Expression of baculovirus P35 prevents cell death in *Drosophila*. Development **120:** 2121–2129.

Hoschuetzky, H., H. Aberle and R. Kemler, 1994 β-catenin mediates the interaction of the cadherin-catenin complex with epidermal growth factor receptor. J. Cell Biol. **127:** 1375–1380.

Hudson, J. B., S. D. Podos, K. Keith, S. L. Simpson and E. L. Ferguson, 1998 The *Drosophila Medea* gene is required downstream of dpp and encodes a functional homolog of human Smad4. Development **125:** 1407–1420.

Kang, D. E., S. Soriano, M. P. Frosch, T. Collins, S. Naruse *et al.*, 1999 Presenilin 1 facilitates the constitutive turnover of beta-catenin: differential activity of Alzheimer's disease-linked PS1 mutants in the beta-catenin-signaling pathway. J. Neurosci. **19:** 4229–4237.

Klingensmith, J., E. Noll and N. Perrimon, 1989 The segment polarity phenotype of *Drosophila* involves differential tendencies toward transformation and cell death. Dev. Biol. **134:** 130–145.

Kurada, K., and K. White, 1998 Ras promotes cell survival in Drosophila by downregulating hid expression. Cell **95:** 319–329.

Levesque, G., G. Yu, M. Nishimura, D. M. Zhang, L. Levesque *et al.*, 1999 Presenilins interact with armadillo proteins including neural-specific plakophilin-related protein and beta-catenin. J. Neurochem. **72:** 999–1008.

Loureiro, J., and M. Peifer, 1998 Roles of Armadillo, a *Drosophila* catenin, during central nervous system development. Curr. Biol. **8:** 622–632.

Mahajan-Miklos, S., and L. Cooley, 1994 The villin-like protein encoded by the Drosophila quail gene is required for actin bundle assembly during oogenesis. Cell **78:** 291–301.

Martin-Blanco, E., A. Gampel, J. Ring, K. Virdee, N. Kirov *et al.*, 1998 *puckered* encodes a phosphatase that mediates a feedback loop regulating JNK activity during dorsal closure in *Drosophila*. Genes Dev. **12:** 557–570.

Martinez Arias, A., 1985 The development of *fused-* embryos of *Drosophila melanogaster*. J. Embryol. Exp. Morph. **87:** 99–114.

McEwen, D. G., R. T. Cox and M. Peifer, 2000 The canonical Wnt and JNK cascades collaborate to promote both dorsal closure and ventral patterning. Development **127** (in press).

Müller, H.-A. J., and E. Wieschaus, 1996 *armadillo*, *bazooka*, and *stardust* are critical for formation of the zonula adherens and maintenance of the polarized blastoderm epithelium in *Drosophila*. J. Cell Biol. **134:** 149–165.

Murayama, M., S. Tanaka, J. Palacino, O. Murayama, T. Honda *et al.*, 1998 Direct association of presenilin-1 with beta-catenin. FEBS Lett. **433:** 73–77.

Neumann, C. J., and S. M. Cohen, 1996 Distinct mitogenic and cell fate specification functions of wingless in different regions of the wing. Development **122:** 1781–1789.

Nishimura, M., G. Yu, G. Levesque, D. M. Zhang, L. Ruel *et al.*, 1999a Presenilin mutations associated with Alzheimer disease cause defective intracellular trafficking of beta-catenin, a component of the presenilin protein complex. Nat. Med. **5:** 164–169.

Nishimura, M., G. Yu and P. H. St. George-Hyslop, 1999b Biology of presenilins as causative molecules for Alzheimer disease. Clin. Genet. **55:** 219–225.

Nüsslein-Volhard, C., and E. Wieschaus, 1980 Mutations affect-

ing segment number and polarity in *Drosophila*. Nature **287:** 795–801.

Pazdera, T. M., P. Janardhan and J. S. Minden, 1998 Patterned epidermal cell death in wild-type and segment polarity mutant Drosophila embryos. Development **125:** 3427–3436.

Peifer, M., D. Sweeton, M. Casey and E. Wieschaus, 1994 *wingless* signal and Zeste-white 3 kinase trigger opposing changes in the intracellular distribution of Armadillo. Development **120:** 369–380.

Polakis, P., 1999 The oncogenic activation of β-catenin. Curr. Opin. Genet. Dev. **9:** 15–21.

Provost, E., and D. L. Rimm, 1999 Controversies at the cytoplasmic face of the cadherin-based adhesion complex. Curr. Opin. Cell Biol. **11:** 567–572.

Raftery, L. A., V. Twombly, K. Wharton and W. M. Gelbart, 1995 Genetic screens to identify elements of the decapentaplegic signaling pathway in Drosophila. Genetics **139:** 241–254.

Sanson, B., P. White and J.-P. Vincent, 1996 Uncoupling cadherin-based adhesion from *wingless* signaling in *Drosophila*. Nature **383:** 627–630.

Schupbach, T., and E. Wieschaus, 1989 Female sterile mutations on the second chromosome of *Drosophila melanogaster*. I. Maternal effect mutations. Genetics **121:** 101–117.

Spradling, A. C., D. Stern, A. Beaton, E. J. Rhem, T. Laverty *et al.*, 1999 The BDGP gene disruption project: single P element insertions mutating 25% of vital *Drosophila* genes. Genetics **153:** 135–177.

Su, T. T., F. Sprenger, P. J. DiGregorio, S. D. Campbell and P. H. O'Farrell, 1998 Exit from mitosis in Drosophila syncytial embryos requires proteolysis and cyclin degradation, and is associated with localized dephosphorylation. Genes Dev. **12:** 1495–1503.

Tao, Y. S., R. A. Edwards, B. Tubb, S. Wang, J. Bryan *et al.*, 1996 β-catenin associates with the actin-bundling protein fascin in a non-cadherin complex. J. Cell Biol. **134:** 1271–1282.

Uemura, T., H. Oda, R. Kraut, S. Hatashi, Y. Kataoka *et al.*, 1996 Zygotic *D* E-cadherin expression is required for the processes of dynamic epithelial cell rearrangement in the *Drosophila* embryo. Genes Dev. **10:** 659–671.

Vucic, D., W. J. Kaiser and L. K. Miller, 1998 Inhibitor of apoptosis proteins physically interact with and block apoptosis induced by Drosophila proteins HID and GRIM. Mol. Cell. Biol. **18:** 3300–3309.

Wang, S. L., C. J. Hawkins, S. J. Yoo, H.-A. J. Müller and B. A. Hay, 1999 The *Drosophila* caspase inhibitor DIAP1 is essential for cell survival and is negatively regulated by HID. Cell **98:** 453–463.

White, K., M. E. Grether, J. M. Abrams, L. Young, K. Farrel *et al.*, 1994 Genetic control of programmed cell death in *Drosophila*. Science **264:** 677–683.

Wieschaus, E., and E. Noell, 1986 Specificity of embryonic lethal mutations in *Drosophila* analyzed in germline clones. Roux's Arch. Dev. Biol. **195:** 63–73.

Wieschaus, E., and C. Nüsslein-Volhard, 1986 Looking at embryos, pp. 199–228 in *Drosophila, A Practical Approach*, edited by D. B. Roberts. IRL Press, Oxford.

Yu, G., F. Chen, G. Levesque, M. Nishimura, D. M. Zhang *et al.*, 1998 The presenilin 1 protein is a component of a high molecular weight intracellular complex that contains beta-catenin. J. Biol. Chem. **273:** 16470–16475.

Zhang, Z., H. Hartmann, V. M. Do, D. Abramowski, C. Sturchler-Pierrat *et al.*, 1998 Destabilization of beta-catenin by mutations in presenilin-1 potentiates neuronal apoptosis. Nature **395:** 698–702.

Zhou, J., U. Liyanage, M. Medina, C. Ho, A. D. Simmons *et al.*, 1997 Presenilin 1 interaction in the brain with a novel member of the Armadillo family. NeuroRep. **8:** 1489–1494.

Communicating editor: K. Anderson

APPENDIX A
Refining strongly interacting regions

Interacting deficiencies	Original region	Defining regions	Interaction
Df(2L)sc19-5; Dp(2;1)B19	25A4-5;25D5-7		Strong
Df(2L)sc19-8; Dp(2;1)B19		24C2-8;25C8-9	+Weak
Df(2L)cl-h3		25D2-4;26B2-5	+Weak
Df(2L)tkv2		25D2-4;25D6-E1	—
[a]**Df(2L)spd**	27D-E;28C		Strong
Df(2L)J136-H52		27C2-9;28B3-4	—
[a]**Df(2L) TE29Aa-11**	28E4-7;29B2-C1		Strong
Df(2L)TW137; Dp(2;2) M(2) m[+]	36C2-4;37B9-C1		Strong
Df(2L)H20		36A8-9;36E1-E2	+Weak
Df(2L)M36Fs5; Dp(2;2)M(2)m[+]		36D1-E1;36F1-37A1	+Weak
Df(2L)TW50		36E4-F1;38A67	—
Df(2R)ST1	42B3-5;43E15-18		Strong
Df(2R)cn9		42E;44C	—
Df(2R)PC4	55C1-3;55E2-4		Strong
Df(2R)P34		55E2-4;56C1-11	—
Df(2R)Pc111B		54F6-55A1;55C1-3	—
Df(2R)017	56F5;56F15; + In56D-E;58E-F		Strong
Df(2R)AA21		56F9-17;57D11-12	—
[b]**Df(3L)W10**	75A6-7;75C1-2	75B8;75F1	Strong
[b]**Df(3L)Cat**	75B8;75F1	75A6-7;75C1-2	Strong
Df(3L)Pc-MK	78A2;78C1-5		Strong
Df(3L)Pc		78C1-5;78C9-D3	—
[c]**Df(3R)Scr**	84A1-2;84B1-2		Strong
Df(3R)WIN11		83E1-2;84A4-5	+Weak
Df(3R)CA3		84F2;85A5-7	+Weak
Df(3R)Tpl10, Tp(3;3)Dfd[rv1]		83C1-2;84B1-2	—
Df(3R)MAP2		84A1-2;84A4-5	—
Df(3R)p712	84D4-6;85B6		Strong
Df(3R)D7		843-5;84F1-2	Strong
Df(3R)D1-BX12	91F1-2;92D3-6		Strong
Df(3R)Cha7		91A;91F5	—
C(4)RM	101-104		Strong
Df(4)M62f		101F1-102B	Strong

Boldface, original deficiency.
[a] These two deficiencies fail to complement.
[b] Narrowed each other.
[c] Interaction most likely more distal than original breakpoints.

APPENDIX B
Weakly interacting regions

Weak Interactors	Breakpoints	% supp.
Df(2L)a1	21B8-C1;21C8-D1	4.8
Df(2L)JS32	23C3-5;23D1-2	3.8
Df(2L)sc19-8; Dp(2;1)B19	24C2-8;25C8-9	3.0
Df(2L)N22-3	30A1-2;30D1-2	5.7
Df(2L)prd1.7	33B2-3;34A1-2	3.8
Df(2L)r10	35E1-2;36A6-7	5.4
Df(2L)H20	36A8-9;36E1-2	4.1
Df(2L)TW84	37F5-38A1;39D3-E1	3.8
Df(2R)M41A4	41A	3.6
In(2R)bw[VDe2L] Cy[R]/In(2LR)Gla	41A-B;42A2-3	3.0
Df(2R)vg135	49A-B;49D-E	3.7
Df(2R)Px2	60C5-6;60D9-10	3.1
Df(2R)ES1	60E6-8;60F1-2	3.0
Df(3L)ZN47	64C;65C	3.3
Df(3L)fz-GF3b	70C1-2;70D4-5	4.2
Df(3R)Hu	86A6-B1;86B3-6 + 84D4-5;84F1-2	4.2
Df(3R)crb87-5	95F7;96A17-18	3.6
Df(3R)B81	99C8;100F5	3.5